ACADEMIC PRESS

Available online at www.sciencedirect.com

SCIENCE DIRECT®

DEVELOPMENTAL BIOLOGY

Developmental Biology 258 (2003) 307–318

www.elsevier.com/locate/ydbio

Myf5 and *MyoD* activation define independent myogenic compartments during embryonic development

Boris Kablar,[a,*] Kirsten Krastel,[b] Shahragim Tajbakhsh,[c] and Michael A. Rudnicki[b]

[a] *Department of Anatomy and Neurobiology, Dalhousie University, 5859 University Avenue, Halifax, NS, Canada B3H 4H7*
[b] *Molecular Medicine Program, Ottawa Health Research Institute, 501 Smyth Road, Ottawa, ON, Canada K1H 8L6*
[c] *Stem Cells and Development, Department of Developmental Biology, Pasteur Institute, 25 rue du Dr. Roux, 75724 Cedex 15, Paris, France*

Received for publication 23 August 2002, revised 27 February 2003, accepted 27 February 2003

Abstract

Gene targeting has indicated that *Myf5* and *MyoD* are required for myogenic determination because skeletal myoblasts and myofibers are missing in mouse embryos lacking both *Myf5* and *MyoD.* To investigate the fate of *Myf5:MyoD*-deficient myogenic precursor cells during embryogenesis, we examined the sites of epaxial, hypaxial, and cephalic myogenesis at different developmental stages. In newborn mice, excessive amounts of adipose tissue were found in the place of muscles whose progenitor cells have undergone long-range migrations as mesenchymal cells. Analysis of the expression pattern of Myogenin-*lacZ* transgene and muscle proteins revealed that myogenic precursor cells were not able to acquire a myogenic fate in the trunk (myotome) nor at sites of *MyoD* induction in the limb buds. Importantly, the Myf5-dependent precursors, as defined by *Myf5*^{nlacZ}-expression, deficient for both *Myf5* and *MyoD,* were observed early in development to assume nonmuscle fates (e.g., cartilage) and, later in development, to extensively proliferate without cell death. Their fate appeared to significantly differ from the fate of MyoD-dependent precursors, as defined by *258/−2.5lacZ*-expression (−20 kb enhancer of *MyoD*), of which a significant proportion failed to proliferate and underwent apoptosis. Taken together, these data strongly suggest that Myf5 and MyoD regulatory elements respond differentially in different compartments.

Keywords: Myf5; MyoD; Lineages; Myogenic precursor cells; Development

Introduction

In vertebrates, four myogenic regulatory factors (MRFs), belonging to a group of basic helix–loop–helix (bHLH) transcription factors, are believed to play a critical function in skeletal muscle cell specification (Weintraub, 1993; Rudnicki and Jaenisch, 1995; Megeney and Rudnicki, 1995; Molkentin and Olson, 1996; Ordahl and Williams, 1998). Null mutations in *Myf5*, *MyoD*, and *Mrf4* result in essentially normal patterning of skeletal muscle tissue (Braun et al., 1992; Rudnicki et al., 1992; Zhang et al., 1995), whereas mutation in *Myogenin* causes a substantial reduction in skeletal muscle tissues (Hasty et al., 1993; Nabeshima et al., 1993). However, newborn mice carrying null mutations in both *MyoD* and *Myf5* genes completely lack myoblasts and skeletal myofibers and die shortly after birth (Rudnicki et al., 1993). Taken together, these results led to the proposal that Myf5 and MyoD (primary MRFs) are required for the determination of skeletal myoblasts, while Myogenin and MRF4 (secondary MRFs) act later as differentiation factors (reviewed by Rudnicki and Jaenisch, 1995; Megeney and Rudnicki, 1995; Kablar and Rudnicki, 2000; Tajbakhsh and Buckingham, 2000).

Presomitic and somitic multipotential mesodermal cells in vertebrates give rise to committed myogenic progenitor cells (also known as premyogenic cells) for the skeletal muscle of the body (trunk and limbs) and some head muscles. More anterior nonsomitic paraxial and prechordal head mesoderm are the source of the remaining head muscles (reviewed by Wachtler and Christ, 1992; Hauschka, 1994; Christ and Ordahl, 1995). Somites, which initially form as

* Corresponding author. Fax: +902-494-1212.
E-mail address: bkablar@dal.ca (B. Kablar).

0012-1606/03/$ – see front matter © 2003 Elsevier Science (USA). All rights reserved.
doi:10.1016/S0012-1606(03)00139-8

epithelial spheres on either side of the neural tube, subsequently become compartmentalized into a dorsal epithelial dermamyotome (dermis and muscle) and a ventral mesenchymal sclerotome (vertebral column and ribs). The dermamyotome is the source of all skeletal myogenic precursor cells within the segmented region of the trunk (Ordahl and Le Douarin, 1992; reviewed by Hauschka, 1994; Christ and Ordahl, 1995).

Recent work has suggested that muscles of the limbs and branchial arches were from migratory precursors that are multipotent prior to MRF expression (Kablar et al., 1999). This is consistent with previous findings (Tajbakhsh and Buckingham, 1994) that MRFs are activated after muscle progenitor cell migration to the limb. Moreover, examination of E10.5 embryos hybridized with a Pax3 probe reveals a normal distribution of Pax3-expressing cells migrating from the dermamyotome into the forelimbs and hindlimbs in *Myf5*$^{-/-}$*:MyoD*$^{-/-}$ embryos, suggesting that Pax3 induction and the subsequent migration of myogenic precursors into the limb are unaffected by the absence of MRF expression (Kablar et al., 1999). In addition, the presence and immunoreactivity to proteoglycan antibody (Glant et al., 1986) of *258/−2.5lacZ*-expressing cells in the cartilage primordia of *Myf5*$^{-/-}$*:MyoD*$^{-/-}$ embryos strongly supports the assertion that muscle progenitor cells are multipotential in the absence of MRF expression.

Analysis of early muscle differentiation in embryos harboring null mutations in either *Myf5* or *MyoD* genes, generated from transgenic mice in which the bacterial *lacZ* gene is under the transcriptional control of a truncated MyoD gene promoter (*MD6.0-lacZ* and *258/−2.5lacZ*), reveals that Myf5 and MyoD genes are not redundant, but that each controls the early specification of distinct muscle cell subpopulations (Kablar et al., 1997, 1998). Based on these studies, two hypotheses can be considered. In the first, Myf5-expressing cells constitute a precursor population from which other cell subpopulations (e.g., MyoD-dependent subpopulation of myoblasts) are later generated (Kablar et al., 1997). In this serial model, myogenic precursor cells first give rise to a population of cells expressing Myf5, followed by differentiation of a subset of cells and creation of a MyoD-dependent subpopulation of myogenic cells (Ordahl and Williams, 1998). In the second hypothesis, diversity among myogenic progenitors exists prior to myogenic specification, resulting in two coexisting Myf5- and MyoD-dependent myogenic precursor cell subpopulations. To investigate this phenomenon further, a detailed analysis of β-galactosidase-stained *Myf5*$^{-/-}$*:MyoD*$^{-/-}$ embryos, generated from *Myf5*^{nlacZ} mice, was performed. The expression pattern and fate of *Myf5nlacZ*-expressing cells deficient for *Myf5* and *MyoD* was examined and compared with the expression pattern and fate of mutant *258/−2.5lacZ*-expressing cells (−20 kb enhancer of *MyoD*) (Kablar et al., 1999). Strikingly, the temporal and spatial pattern of Myf5-*lacZ* versus MyoD-*lacZ* expression did not overlap. Therefore, we conclude that two parallel pathways activate and maintain *Myf5* and *MyoD* gene expression from the earliest stages of somite development.

Materials and methods

Interbreeding and collection of embryos

Embryos lacking both *Myf5* and *MyoD* were derived by a two-generation breeding scheme. First, *MyoD*$^{-/-}$ mice were bred with *Myf5*$^{+/-}$ mice to generate *Myf5*$^{+/-}$*: MyoD*$^{+/-}$ mice. Second, *Myf5*$^{+/-}$*:MyoD*$^{+/-}$ mice were interbred to obtain embryos of 9 different genotypes. Transgenic *Myo1565lacZ* mice, generated with 1.565 kb of 5′ *Myogenin* sequence linked to the *lacZ* transgene, were kindly provided by E.N. Olson (Cheng et al., 1993). These transgenic mice were separately bred with mice heterozygous for both the *Myf5* and *MyoD* mutant alleles (Rudnicki et al., 1993). In addition, the *Myf5*^{nlacZ} knock-in mice, in which the *nlacZ* reporter gene is introduced into the *Myf5* locus by homologous recombination (Tajbakhsh et al., 1996), were used. *Myf5*^{nlacZ} knock-in mice were also bred with *MyoD*$^{-/-}$ mice (Rudnicki et al., 1992) to generate *Myf5*^{nlacZ}/+:*MyoD*$^{+/-}$ mice. *Myf5*^{nlacZ}/+*:MyoD*$^{+/-}$ mice were interbred to obtain embryos of 9 different genotypes. Finally, the *258/−2.5lacZ* transgenic mice, that carry a construct in which the 258-bp core of the −20-kb *MyoD* enhancer is linked to 2.5 kb of *MyoD* sequence upstream of the transcription start site upstream of the *lacZ* gene (Goldhamer et al., 1995), were used. These *lacZ* transgenic mice were bred in the same way as described for *Myf5*^{nlacZ} (Kablar et al., 1999). Embryos and the fetal portion of the placenta were collected by cesarean section on embryonic day (E) 10.5, E11.5, and E18.5, and embryos were prepared for hematoxylin–eosin (HE) or eosin staining, oil red-O staining, whole-mount β-galactosidase staining, immunohistochemistry, and whole-mount TUNEL analysis, as described below. Genomic DNA was isolated from the fetal portion of the placenta by using the procedure of Laird et al. (1991). Embryos were genotyped by Southern analysis (Sambrook et al., 1989) of placental DNA using *Myf5*, *MyoD*, and *lacZ* specific probes as described previously (Rudnicki et al., 1993). Care of animals was in accordance with institutional guidelines.

β-Galactosidase staining

β-Galactosidase staining was performed as described by Kablar et al. (1999). Embryos were fixed 1–2 h (2% paraformaldehyde, 0.2% glutaraldehyde, 0.1 M phosphate buffer, pH 7.4, and 2 mM $MgCl_2$), and washed twice for 30 min in solution A (0.1 M phosphate buffer, pH 7.4, 2 mM $MgCl_2$, 0.1% sodium deoxycholate, 0.2% Nonidet P-40) and then washed twice, for 30 min in solution B (0.1 M phosphate buffer, pH 7.4, 2 mM $MgCl_2$, 0.01% sodium deoxycholate, 0.2% Nonidet P-40). β-Galactosidase was

detected by overnight incubation at 37°C in 1.0 mg/ml X-gal (5-bromo-4-chloro-3-indolyl-β-D-galactoside), 5 mM potassium ferricyanide, and 5 mM potassium ferrocyanide. Embryos were washed twice for 1 h at room temperature in phosphate-buffered saline (PBS), post-fixed overnight, dehydrated, and stored at 4°C in 70% ethanol. Whole embryos were photographed in 70% ethanol by using a Zeiss dissecting microscope.

Immunohistochemistry

Immunohistochemistry was performed as previously described (Kablar et al., 1997, 1998) on paraffin-embedded 4-μm sections with mouse monoclonal anti-desmin antibody D33 (1:100, DAKO), mouse monoclonal anti-nestin antibody Rat-401 (1:4, Developmental Studies Hybridoma Bank), mouse monoclonal anti-myosin heavy chain (MHC) antibody MF20 (1:10, Bader et al., 1982), mouse monoclonal anti-myocyte nuclear factor (MNF) antibody (1:50, Garry et al., 1997), mouse monoclonal anti-Proliferating Cell Nuclear Antigen (PCNA) antibody (1:400, DAKO), rabbit polyclonal anti-Myf-5 antibody C-20 (1:100, Santa Cruz), rabbit polyclonal anti-MyoD antibody M-318 (1:50, Santa Cruz), and rabbit polyclonal anti-Myogenin (myg) antibody m-225 (1:20, Santa Cruz).

In situ TUNEL analysis

To detect apoptotic nuclei in situ by TUNEL (Gavrieli et al., 1992), we employed the ApopTag detection system (Genzyme). Whole embryos (E10.5) or transverse sections (E10.5; E14.5) were incubated with terminal deoxynucleotydil transferase (TdT enzyme) diluted in the reaction buffer. The enzyme catalyzes a template-independent addition of deoxyribonucleotide triphosphate to the 3′-OH ends of double- or single-stranded DNA. The incorporated nucleotides form a random heteropolymer of digoxygenin-11-dUTP and dATP that has a reaction site for anti-digoxigenin antibody carrying a conjugated peroxidase enzyme. The localized peroxidase enzyme was visualized by a chromogenic reaction with AEC (3-amino-9-ethylcarbazole, Sigma). Whole embryos were photographed in 70% ethanol by using a Zeiss dissecting microscope. For morphometric analysis of apoptotic nuclei, the embryos were embedded in paraffin and 10-μm serial sections mounted on slides and counterstained with eosin.

Morphometry

Apoptotic nuclei counts from whole-mount TUNEL-stained embryos were made in every 10th section corresponding to the forelimb level of an embryo. The data presented are the actual cell counts multiplied with 10 and then divided by the total number of sections per region to yield apoptotic nuclei per section, as described by Kablar and Rudnicki (1999). Apoptotic nuclei in TUNEL-stained transverse sections were counted under the magnification of 1000× in 7 randomly chosen microscopic fields with the area of 9 mm^2 per field (Inanlou and B.K., unpublished data).

The oil red-O-positive lipid droplets were counted in 100 microscopic fields. Each field measured 1 mm^2 (total of 1 cm^2), and the counts were made at a magnification of 1000×.

To evaluate the significance of differences in the number of lipid droplets or apoptotic nuclei between wild-type and compound-mutant embryos, the mean and standard error of the mean (s.e.m.) were calculated for counts of each genotype and *t* tests were performed. All *P* values are two-sided.

Results

Absence of skeletal muscle and expanded adipose tissue in newborn mice lacking both Myf5 and MyoD genes

As previously reported by Rudnicki et al. (1993), *Myf5*$^{-/-}$*:MyoD*$^{-/-}$ newborn mice (E18.5) completely lack myoblasts and differentiated skeletal muscle in their head, trunk, and limbs. Previous analysis of early muscle differentiation in embryos harboring null mutations in either *Myf5* or *MyoD* genes revealed that *Myf5* and *MyoD* play unique developmental roles. *Myf5* plays a unique role in development of muscles arising after translocation of epithelial dermomyotome cells along the edge of the somite to the subjacent myotome (for example, back and intercostal muscle precursors by migration). *MyoD* plays a unique role in the development of muscles arising from migratory precursor cells (for example, limb and branchial arch muscles, tongue, and diaphragm; Kablar et al., 1997, 1998).

To investigate the fate of myogenic precursor cells that normally give rise to Myf5-dependent muscles and those that normally give rise to MyoD-dependent muscle groups, we analyzed *Myf5*$^{-/-}$*:MyoD*$^{-/-}$ newborn mice at eight different anatomical locations: external ocular muscles, facial muscles, tongue, forelimbs, diaphragm, back muscles, intercostal muscles, and abdominal wall muscles. We found that in the place of back, intercostal, and abdominal wall muscles (all epithelial in their origin, i.e., do not form from migrating muscles progenitors; Ordahl and Williams, 1998), an excessive amount of adipose tissue was formed (Fig. 1, and data not shown). The oil red-O staining demonstrated a 4.3 times increase in the number of lipid droplets in the adipose tissue formed in the intercostal region of double mutant embryos (i.e., 104 ± 13 in wild-type versus 449 ± 18 in double mutant, per 1 cm^2). Unfortunately, the adipose tissue did not express the *nlacZ* transgene and, therefore, we were unable to demonstrate a coexpression between *nlacZ* and oil red-O. It remains possible that the *nlacZ*-expression was rapidly downregulated as muscle progenitor cells change fate to fat. Alternatively, in this case, there is no

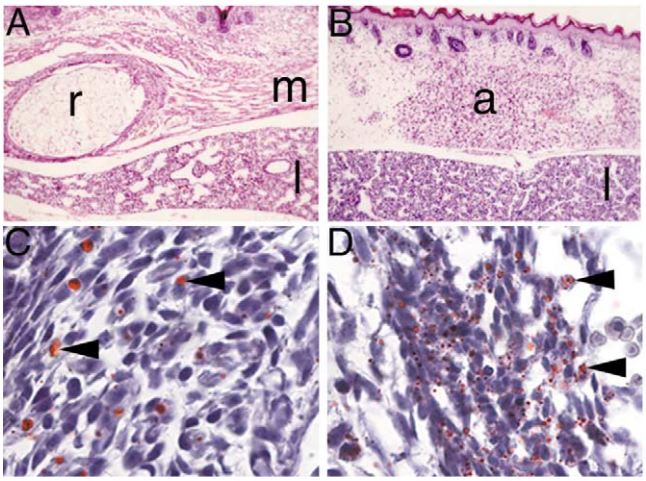

Fig. 1. Newborn (E18.5) *Myf5*$^{-/-}$*:MyoD*$^{-/-}$ embryos lack all skeletal muscle and have excess of adipose tissue. Transverse sections of E18.5 wild-type (A, C) and *Myf5*$^{-/-}$*:MyoD*$^{-/-}$ embryos (B, D) stained with HE (A, B) and oil red-O (C, D) reveal that, in the place of intercostal muscles (m in A; arrowheads in C show normal amount of lipid droplets in the skeletal muscle tissue), an excessive amount of adipose tissue is visible in mutant embryos only (a, in B; arrowheads in D show lipid droplets whose number is significantly increased in the tissue replacing intercostal muscle). Abbreviations: a, adipose tissue; 1, lung, m, intercostal skeletal muscle, r, rib primordium (note that mutant embryos have a rib defect). Magnification, 100 × (A, B), 1000 × (C, D).

change in cell fate, and our findings simply represent a physiological expansion of endogenous fat tissue in the place of the missing muscle tissue.

By contrast, in the place of ocular, facial, and limb muscle as well as the tongue and the diaphragm (all arise from long-range migratory myogenic precursor cells; Ordahl and Williams, 1998), adipose tissue was not observed (data not shown). An approximately normal amount of loose connective tissue was observed in the place of skeletal muscle in the region of mutant forelimbs (data not shown). In addition, it was possible to observe cleft palate (*palatoshisis*), somewhat shorter long bones of the limbs and a rib defect, as previously described for Myf5 null embryos (Braun et al., 1992).

Absence of Myogenin and muscle proteins in the trunk of Myf5$^{-/-}$*:MyoD*$^{-/-}$ *embryos*

To investigate whether myogenic precursor cells are able to differentiate into a small number of myocytes in the absence of primary MRFs during early stages of embryonic development, we studied the expression pattern of Myogenin-*lacZ* trangene in E11.5 embryos that were deficient for *Myf5* and *MyoD* genes (Fig. 2). In wild-type *Myo1565lacZ* transgenic embryos, a strong *lacZ* expression was detected in differentiated myocytes throughout the entire myotome all along the embryonic axis as well as in the extramyotomal muscle primordia of the ventral neck area, branchial arches, and forelimbs (Cheng et al., 1993; Fig. 2A). A similar pattern of expression was also described by Sassoon et al. (1989) for endogenous *Myogenin* mRNA. In *MyoD*$^{-/-}$ embryos, myotomal expression of Myogenin-*lacZ* transgene was somewhat altered (Fig. 2B) compared with wild-type embryos. Expression of *lacZ* appeared uneven in intensity and the extent of expression particularly at the dorsal edge varied between myotomes. This corresponds to a reduction in the amount of differentiated cells in these embryos. Consistent with the expression pattern of Myogenin protein (Kablar et al., 1997), the Myogenin-*lacZ* transgene was not expressed in the forelimbs and branchial arches. In E11.5 *Myf-5*$^{-/-}$ embryos, Myogenin-*lacZ* expression was greatly reduced in extent and intensity (Fig. 2C), compared with wild-type and *MyoD*$^{-/-}$ mice. *lacZ* expression was only observed in the dorsal and ventral portions of myotomes with a large gap present in the central myotomal region. This corresponds to the aberrant pattern of muscle progenitor cells observed previously with the *Myf5*^{nlacZ} (Tajbakhsh et al., 1996). Consistent with the expression pattern of Myogenin protein (Kablar et al., 1997), *lacZ* transgene was found in the forelimbs and branchial arches. In *Myf5*$^{-/-}$*:MyoD*$^{-/-}$ embryos, Myogenin-*lacZ* expression was observed (Fig. 2D). No ectopic expression was detected in any of the genotypes studied for this transgene (Fig. 2A–D). Therefore, in the *Myf5:MyoD* mutants, myogenic precursor cells do not acquire a myoblast phenotype.

To investigate further if any myogenic precursor cells form and differentiate into skeletal myoblasts in the myotomes of *Myf5*$^{-/-}$*:MyoD*$^{-/-}$ embryos, we employed immunohistochemistry on transverse section of wild-type and mutant embryos at E11.5 (Fig. 3). A panel of antibodies reactive with proteins also expressed in myogenic precursor cells (Myf5, MyoD, and MNF; Garry et al., 1997), in myoblasts (Myogenin, nestin, and desmin), and in differentiated myotubes (MHC) was employed. Desmin and nestin are intermediate filaments expressed in both proliferating myoblasts and newly formed differentiating myocytes, whereas MHC is expressed exclusively in terminally differentiated myotubes and myofibers (Bischoff, 1994; Hauschka, 1994).

Transverse sections of E11.5 wild-type embryos at the level of forelimbs stained with anti-Myf5, anti-MyoD, and anti-MNF antibody revealed presence of myogenic precursor cells in the region of the myotome (Fig. 3A, C, and E). Adjacent sections stained with anti-myg, anti-nestin, and anti-desmin antibody revealed presence of myoblasts and differentiated myocytes in the myotome at the forelimb level (Fig. 3G, I, and K). Sections stained with anti-MHC antibody revealed presence of terminally differentiated myotubes and myofibers in the region of the myotome (Fig. 3M). Transverse sections of E11.5 *Myf5*$^{-/-}$*:MyoD*$^{-/-}$ embryos at the level of forelimbs did not stain with anti-Myf5, anti-MyoD, and anti-MNF antibody, revealing absence of Myf5-, MyoD- (and correct genotyping), or MNF-expressing myogenic precursor cells in the region of the myotome (Fig. 3B, D, and F). Companion sections did not stain with anti-myg, anti-nestin, and anti-desmin antibody, revealing

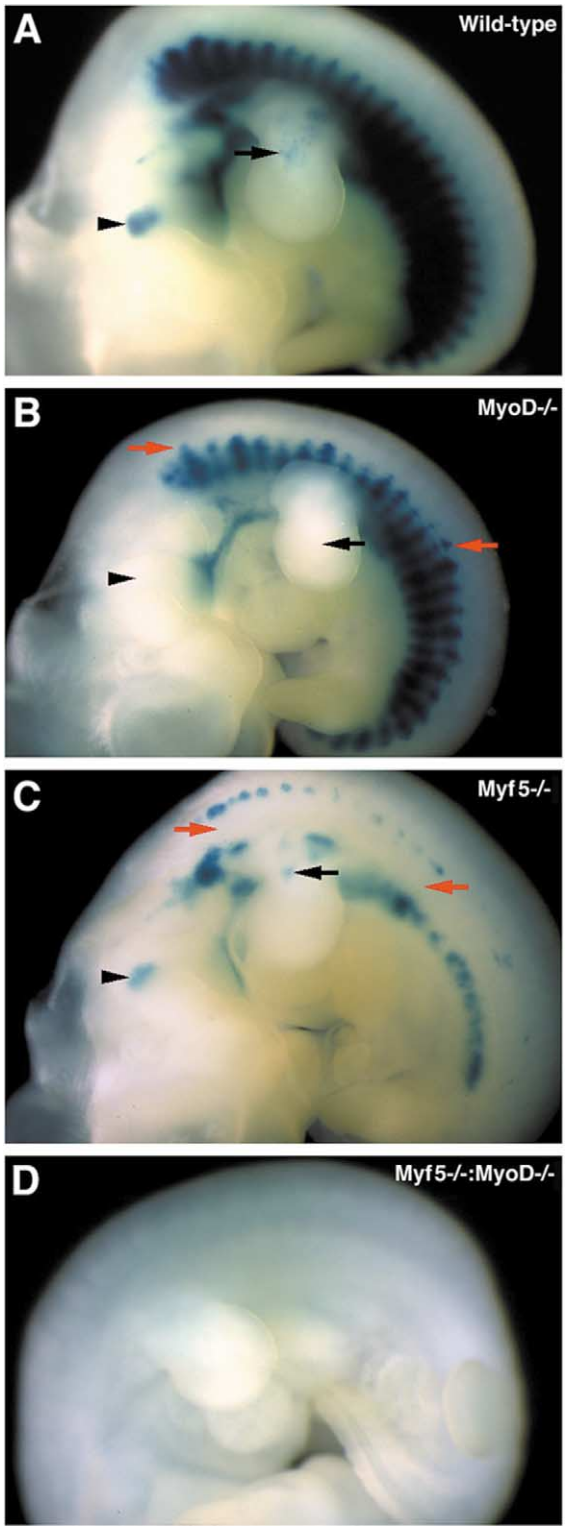

Fig. 2. The expression of Myogenin-*lacZ* transgene in E11.5 $Myf5^{-/-}$:$MyoD^{-/-}$ embryos is totally abolished. Wild-type *Myo1565lacZ* transgenic embryos (A) have a strong *lacZ* expression throughout the entire myotome, the ventral neck area, branchial arches (arrowhead in A), and forelimbs (arrow in A). In E11.5 $MyoD^{-/-}$ embryos, myotomal expression of Myogenin-*lacZ* transgene appears uneven in intensity and the extent at the dorsal edge (red arrows in B). *lacZ* transgene is not expressed in the forelimbs (black arrow in B) and branchial arches (arrowhead in B). In E11.5 $Myf5^{-/-}$ embryos, *lacZ* expression is greatly reduced in extent and intensity (C) and is only observed in the dorsal and ventral portions of myotomes with a large gap present in the central myotomal region (red arrows in C). *lacZ* transgene is found in the forelimbs (black arrow in C) and branchial arches (arrowhead in C). In $Myf5^{-/-}$:$MyoD^{-/-}$ embryos, no *Myo1565lacZ* expression is observed (D). No ectopic expression is detected in any of the genotypes studied for this transgene (A–D).

absence of myoblasts and differentiated myocytes in the myotome at the forelimb level (Fig. 3H, J, and L). Sections that did not stain with anti-MHC antibody revealed absence of terminally differentiated myotubes and myofibers in the region of the myotome (Fig. 3N). Sections of both wild-type and mutant embryos stained with anti-MNF and anti-nestin also stained neuroepithelial derivatives (Fig. 3E, F, I, and J).

The sections made at E10.5, as well as sections in the forelimbs, gave the same results (data not shown).

Therefore, we conclude that, in these *Myf5:MyoD* mutants, myogenic precursor cells can not undergo their normal developmental program that leads to the acquisition of a myogenic fate. Presumably, these precursor cells remain either developmentally arrested, undergo programmed cell death, or change their fate.

Increased apoptosis in the somites and forelimbs of $Myf5^{-/-}$:$MyoD^{-/-}$ embryos

To investigate whether myogenic precursor cells undergo programmed cell death in the absence of primary MRFs, we performed whole-mount in situ TUNEL analysis on wild-type (Fig. 4A–D) and $Myf5^{-/-}$:$MyoD^{-/-}$ (Fig. 4E–H) E10.5 embryos. This analysis revealed increased levels of programmed cell death in both the somite and the forelimbs. Morphometric analysis of serial transverse sections revealed a statistically significant ($P < 0.001$) difference between the number of apoptotic nuclei in wild-type and double mutant somite (19 ± 5 per section in wild-type embryos and 32 ± 7 per section in mutant embryos; compare Fig. 4C and Fig. 4G) and limbs (14 ± 6 per section in wild-type embryos and 27 ± 5 per section in mutant embryos; compare Fig. 4D and Fig. 4H). High level of apoptosis was observed in apical forelimb bud ridge of both genotypes (Fig. 4D and H). In the wild-type E10.5 embryo, the number of cells that express MyoD is 138 ± 19 per section.

To determine whether apoptosis affected differently *lacZ*-expressing cells in $Myf5^{nlacZ/nlacZ}$:$MyoD^{-/-}$ embryos in comparison with $Myf5^{-/-}$:$MyoD^{-/-}$ embryos expressing *258/− 2.5lacZ* (−20 kb enhancer of *MyoD*), we performed TUNEL analysis on transverse sections. In both the myotome and the forelimbs, the number of apoptotic cells (co-expressed with *lacZ*) was significantly higher ($P < 0.001$) in E10.5 $Myf5^{nlacZ/nlacZ}$:$MyoD^{-/-}$ embryos in comparison with the $Myf5^{nlacZ/+}$ control (Fig. 4I and J, the myotome, 12 ± 3 per section in control embryos and 27 ± 4 per section in mutant embryos; Fig. 4K and L, the forelimbs, 11 ± 7 per

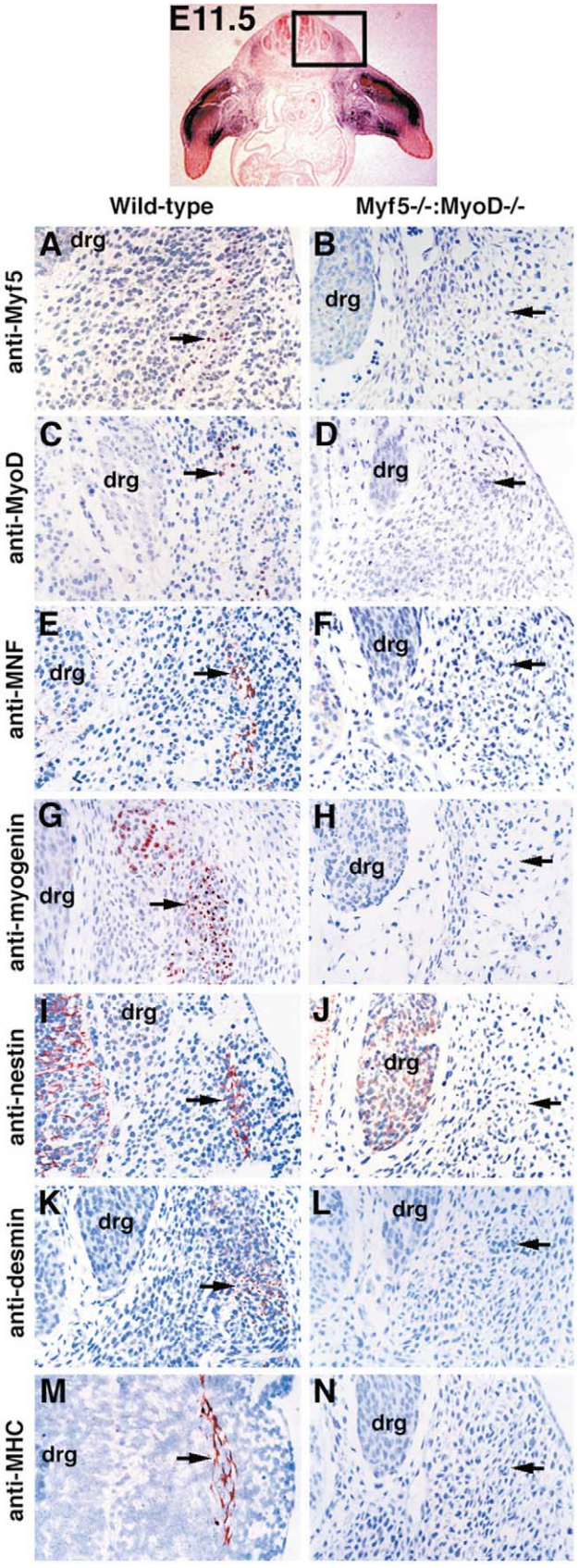

Fig. 3. Transverse sections of E11.5 wild-type (A, C, E, G, I, K, M) and *Myf5*$^{-/-}$*:MyoD*$^{-/-}$ (B, D, F, H, J, L, N) embryos at the level of forelimbs, stained with anti-Myf5 (A, B), anti-MyoD (C, D), anti-MNF (E, F), anti-Myogenin (G, H), anti-nestin (I, J), anti-desmin (K, L), and anti-MHC (M, N) antibody. No antibody marks the region of mutant myotome (arrows in B, D, F, H, J, L, N), while the expected staining pattern is visible in the wild-type myotome (arrows in A, C, E, G, I, K, M). Abbreviations: drg, dorsal root ganglia. Magnification, 200×.

section in control embryos and 23 ± 5 per section in mutant embryos). No difference (in comparison to control, $P > 0.05$) was found when the same analysis was performed on wild-type (control) and *Myf5*$^{-/-}$*:MyoD*$^{-/-}$ embryos expressing *258/−2.5lacZ* (the myotome, 6 ± 3 per section in control embryos and 3 ± 4 per section in mutant embryos; the forelimbs, 4 ± 7 per section in control embryos and 6 ± 5 per section in mutant embryos).

Therefore, we conclude that, in the absence of Myf5 and MyoD, muscle progenitor cells undergo programmed cell death from early stages of development.

Muscle progenitor cell fate and somite compartmentalization are affected in Myf5:MyoD mutants

To study muscle progenitor cell fate and the process of somite compartmentalization, we employed the *Myf5*^{nlacZ} knock-in mice, in which the *nlacZ* reporter gene is introduced into the *Myf5* locus by homologous recombination (Tajbakhsh et al., 1996). Previously, it was shown that *nlacZ*-expressing muscle progenitor cells are present in the dermomyotome of *Myf5* null embryos, where they undergo aberrant migration and are found in dermal precursors to express *Dermo-1* and in sclerotome to coexpress *scleraxis* (Tajbakhsh et al., 1996). Consistently, in *Myf5*$^{nlacZ/nlacZ}$*: MyoD*$^{-/-}$ embryos, muscle progenitors that have activated *Myf5* are present, but the pattern of β-galactosidase staining in mutant embryos (Figs. 5B, D, F, H, and J and 6B, D, F, H, J, and L) is substantially different from the heterozygous pattern (Figs. 5A, C, E, G, and I, and 6A, C, E, G, I, and K).

At earlier stages (E11.5 and E12.5), the pattern of β-galactosidase staining between heterozygous and mutant embryos is not different due to the shape of the dermomyotome (Fig. 5A–D, arrowheads in B), but is due to the fact that progenitor cells are developmentally arrested and are retained outside and adjacent to the dorsal and ventral dermomyotome lips. In transverse tissue sections (E12.5), it was possible to note that, like in the heterozygous myotomes (Fig. 6A and E, m), *nlacZ*-expressing cells of mutant embryos delaminated from the dermomyotome and lost their columnar shape to become mesenchymal, at both the level of the limbs (Fig. 6B, m) and at the level of the tail (Fig. 6F, m). However, some *nlacZ*-expressing mutant cells were found dorsally, in the columnar dermatome (Fig. 6F, d) and ventrally in the sclerotome (Fig. 6F, s). Heterozygous dermatome (Fig. 6E, d) and sclerotome (Fig. 6E, s) did not contain *nlacZ*-expressing cells. Occasionally, *nlacZ*-expressing cells were also found in the dermis of mutant forelimbs (Fig. 6D, arrowhead). At later developmental

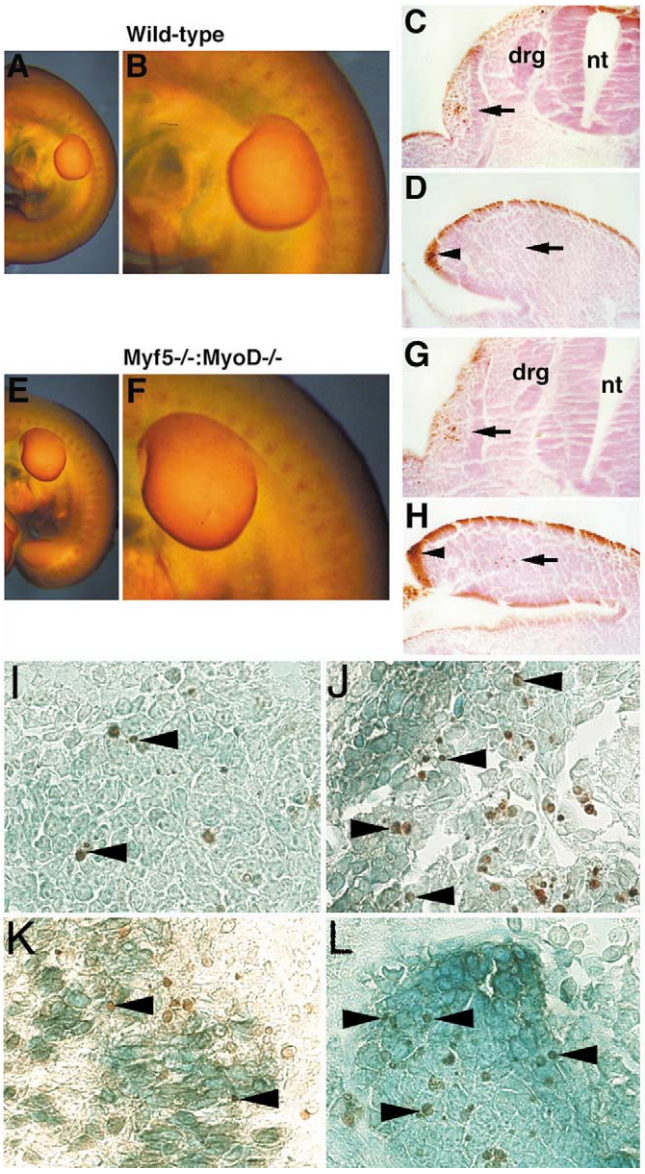

Fig. 4. Muscle progenitor cells undergo programmed cell death from early developmental stages in the absence of Myf5 and MyoD. Whole-mount TUNEL detection of apoptosis is performed in E10.5 wild-type (A–D) and *Myf5*$^{-/-}$*:MyoD*$^{-/-}$ (E–H) embryos. In both the dermomyotome (arrows in C and G) and the forelimbs (arrows in D and H), a significantly elevated occurrence of programmed cell death is observed in *Myf5*$^{-/-}$*:MyoD*$^{-/-}$ embryos. Morphometric analysis of serial transverse sections reveals a statistically significant difference between the number of apoptotic nuclei in wild-type and mutant dermomyotome and limbs (see Results). High level of apoptosis is observed in apical forelimb bud ridge of both genotypes (arrowheads in D and H). TUNEL analysis on transverse sections is performed to assess apoptosis in E10.5 *Myf5*$^{nlacZ/nlacZ}$*:MyoD*$^{-/-}$ embryos (J, L) in comparison with the *Myf5*$^{nlacZ/+}$ control (I, K). In both the myotome (I, J) and the forelimbs (K, L), the number of apoptotic cells (coexpressed with *lacZ*, arrowheads in I, J) was significantly higher in E10.5 *Myf5*$^{nlacZ/nlacZ}$*:MyoD*$^{-/-}$ embryos in comparison with the control (see Results). Abbreviations: drg, dorsal root ganglia; nt, neural tube. Magnification (C, D, G, H), 200×.

ages (E13.5–E15.5), the pattern of β-galactosidase staining between heterozygous and mutant embryos differed significantly. While the staining in heterozygous embryos was spreading at the sites of skeletal muscle development (Fig. 5E, G, and I), the pattern of β-galactosidase expression in mutant embryos remained restricted first to the dorsal- and ventral-most myotomes and to the limbs (Fig. 5F), followed by its further restriction to the dorsal dermomyotomal regions and limbs (Fig. 5H and J).

To further our understanding of muscle progenitor cell fate in *Myf5:MyoD* mutants, we performed immunohisto-

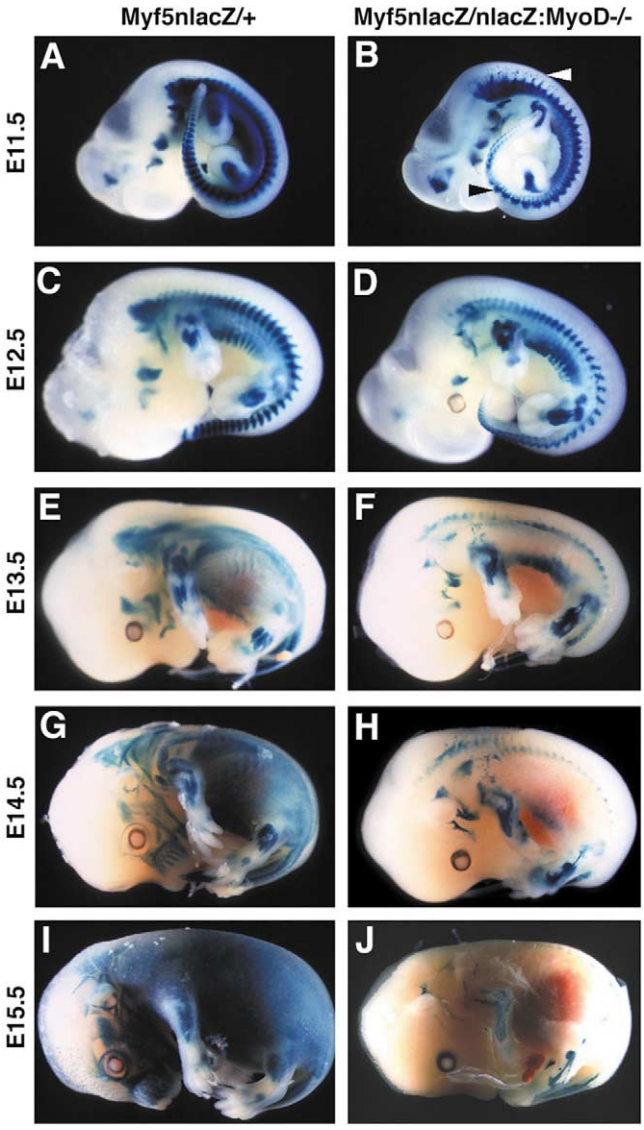

Fig. 5. The expression pattern of *Myf5*^{nlacZ} transgene in heterozygous E11.5 (A), E12.5 (C), E13.5 (E), E14.5 (G), E15.5 (I), and *Myf5*$^{nlacZ/nlacZ}$*:MyoD*$^{-/-}$ E11.5 (B), E12.5 (D), E13.5 (F), E14.5 (H), E15.5 (J) embryos, as revealed by whole-mount β-galactosidase staining. At earlier stages (E11.5 and E12.5; A–D), the pattern of β-galactosidase staining between heterozygous and mutant embryos is distinguished by the aberrant pattern of muscle progenitor cell accumulation (arrowheads in B). At later developmental ages (E13.5–E15.5; E–J), the staining in heterozygous embryos extends to the sites of skeletal muscle development (E, G, I). By contrast, the mutant pattern of β-galactosidase expression remains restricted to the dorsal and ventral tips of the somites and to the limbs (F), followed by its further restriction to the dorsal myotomal tips and limbs (H, J).

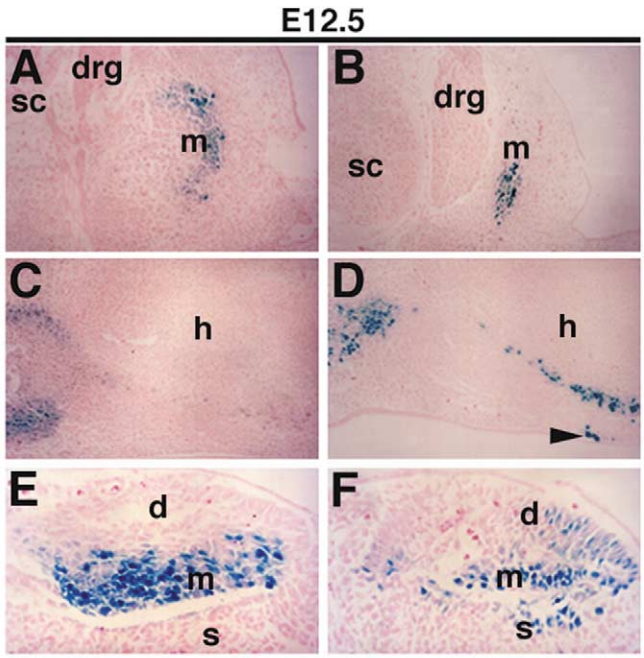

6 Myf5nlacZ/+ Myf5nlacZ/nlacZ:MyoD-/-

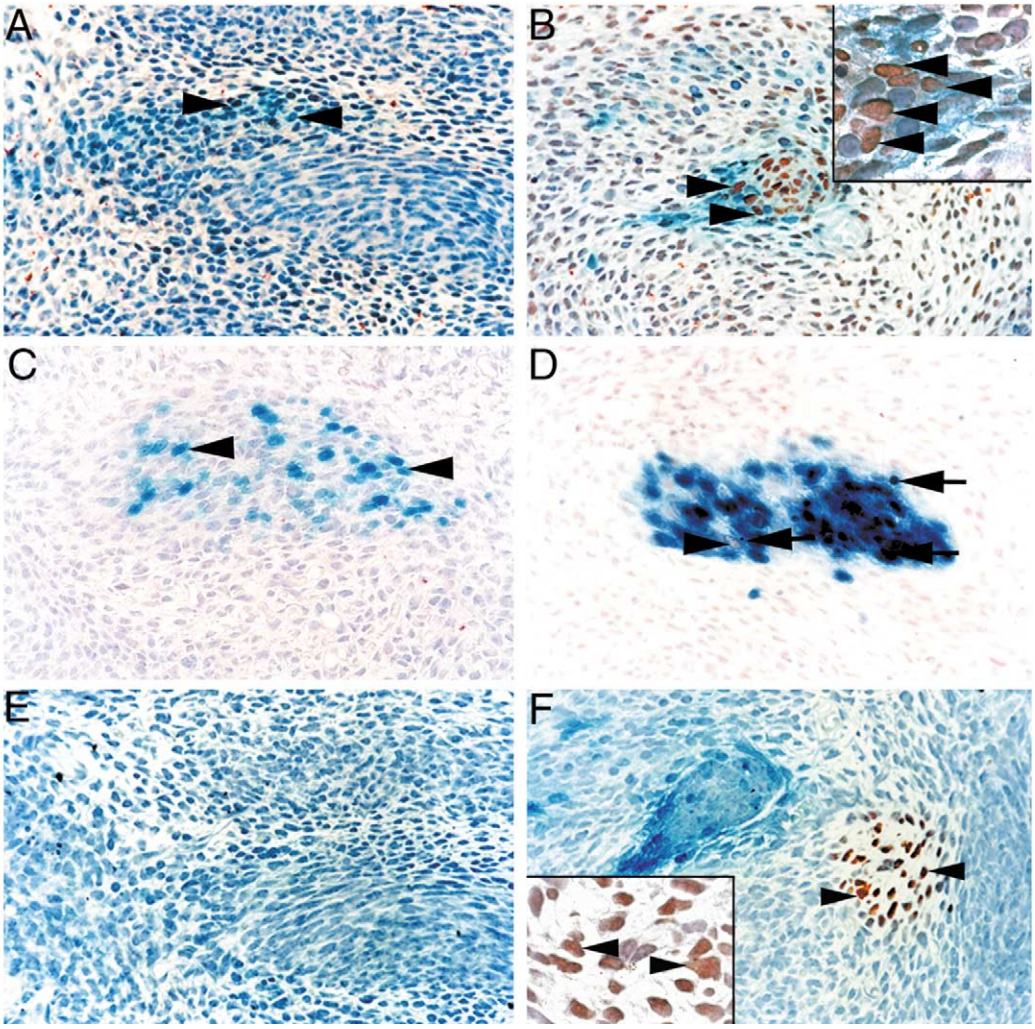

7

chemistry against anti-proliferating cell nuclear antigen (PCNA) antibody. PCNA functions as a cofactor for DNA polymerase delta in S-phase of the cell cycle. In transverse forelimb sections from *Myf5*^{nlacZ} heterozygous (Fig. 7A) and *258/−2.5lacZ* (−20 kb enhancer of *MyoD*) (Fig. 7C) E14.5 embryos, it was not possible to observe expression of PCNA in the nuclei expressing *lacZ* (Fig. 7A and C, arrowheads). Surprisingly, immunostaining of transverse forelimb sections from *Myf5*$^{nlacZ/nlacZ}$*:MyoD*$^{-/-}$ mutant (Fig. 7B) E14.5 embryos revealed that *lacZ*-expressing cells were also PCNA-positive (Fig. 7B, arrowheads), whereas in *258/−2.5lacZ* double mutant (*Myf5*$^{-/-}$*:MyoD*$^{-/-}$) embryos, coexpression of PCNA and β-galactosidase was a very rare observation (Fig. 7D, arrowheads).

Previously, double labeling of matched wild-type and compound mutant sections of embryos with β-galactosidase and in situ detection of apoptosis (TUNEL) revealed a massive programmed cell death of cells stained with *258/−2.5lacZ* in double mutant embryos (Kablar et al., 1999). By contrast, TUNEL detection in *Myf5*$^{nlacZ/nlacZ}$*:MyoD*$^{-/-}$ E14.5 embryos revealed that β-galactosidase-expressing cells were not undergoing programmed cell death (Fig. 7F) and that a different group of cells, not expressing *Myf5*^{nlacZ}, was undergoing apoptosis in double mutant forelimbs (Fig. 7F, arrowheads). Consistently, no apoptosis was observed in cells expressing *Myf5*^{nlacZ}/+ E14.5 embryos (Fig. 7E).

Taken together, these results indicate that in the absence of Myf5 and MyoD muscle progenitor cells delaminate from the dermomyotome to become mesenchymal. These cells encounter multiple cell fate decisions: they remain multipotent and affect somite compartmentalization in the trunk, remain highly proliferative and developmentally arrested, or change fate into (dermis) or cartilage or undergo programmed cell death.

Discussion

Mounting evidence supports the notion that *Myf5* and *MyoD* play unique roles in the development of epaxial (originating in the dorsomedial half of the somite, e.g., back muscles) and hypaxial (originating in the ventrolateral half of the somite, e.g., limb and body wall muscles) musculature, respectively (Kablar et al., 1997, 1998; Ordahl and Williams, 1998). Analysis of *Myf5*$^{-/-}$*:MyoD*$^{-/-}$ newborn mice revealed that, in the place of back, intercostal, and abdominal wall muscles, all arising from short-range migrations (Ordahl and Williams, 1998; Tajbakhsh and Buckingham, 2000), an excessive amount of adipose tissue was formed. By contrast, in the place of ocular, facial, limb muscle, tongue, and diaphragm, arising from migratory mesenchymal myogenic progenitor cells (Ordahl and Williams, 1998), adipose tissue was not found. Interestingly, expression of *lacZ* in ribs and nonmuscle cells is observed in *Myf5*^{nlacZ} knock in mice in the absence of *Myf5* (Tajbakhsh et al., 1996), as well as in the absence of both *Myf5* and *MyoD*. In addition, some cells of the *Myf5*$^{-/-}$*:MyoD*$^{-/-}$ cartilage primordia coexpress MyoD-*lacZ* (*258/−2.5lacZ*) and anti-fetal cartilage proteoglycan protein (Kablar et al., 1999), suggesting that myogenic precursor cells change not only their position, but also their identity in a mutant embryo. In the present study, we were not able to demonstrate colocalization of the adipose marker and β-galactosidase. Interestingly, we note that the expansion in adipose tissue was observed only in the trunk, but not in the regions where migratory muscle cell progenitors give rise to skeletal muscle.

Myogenic precursor cells initially arise in the epaxial epithelial somite, followed by a substantial contribution mainly from epaxial and hypaxial edges of the dermomyotome (Tajbakhsh and Spörle, 1998; Tajbakhsh and Buckingham, 2000). As mentioned previously, *Myf5*$^{-/-}$*:MyoD*$^{-/-}$ E18.5 embryos and newborns lack all skeletal muscle (Rudnicki et al., 1993), indicating that *Myf5* and *MyoD* are key regulators of myogenic determination. However, it remained unclear whether the precursor myoblast population did not form, did not differentiate, or just did not survive in the *Myf5*$^{-/-}$*:MyoD*$^{-/-}$ embryo. It was later shown that, prior to MyoD activation, muscle progenitor

Fig. 6. The expression pattern of *Myf5*^{nlacZ} transgene in *Myf5*^{nlacZ}/+ E12.5 (A, C, E) and *Myf5*$^{nlacZ/nlacZ}$*:MyoD*$^{-/-}$ E12.5 (B, D, F) embryos, in transverse sections counterstained with eosin. *nlacZ*-expressing cells of mutant embryos delaminate from the dermomyotome (d in F) and lose their columnar shape to become mesenchymal myotome at the level of the limbs (m in B) and at the level of the tail (m in F). In addition, some *nlacZ*-expressing mutant cells are found in the dermomyotome (d in F) and sclerotome (s in F). Heterozygous dermomyotome (d in E) and sclerotome (s in E) does not contain *nlacZ*-expressing cells. *nlacZ*-expressing cells are also found in the dermis of mutant forelimbs (D, arrowhead). Please note that the same letters are used for labeling of the corresponding regions of the myotome (m) and the dermomyotome (d) in the double mutant embryos, although double mutant embryos do not form the myotome and the dermomyotome. Abbreviations: d, dermamyotome; drg, dorsal root ganglia; h, humeral primordium; m, myotome; s, sclerotome; sc, spinal cord. Magnification, 400×.

Fig. 7. Immunostaining against anti-PCNA antibody (A–D) and in situ detection of apoptosis (TUNEL) (E, F) in transverse forelimb sections from E14.5 *Myf5*^{nlacZ}/+ (A, E), E14.5 *258/-2.5lacZ* wild-type (C), E14.5 *258/−2.5lacZ* double mutant (*Myf5*$^{-/-}$*:MyoD*$^{-/-}$) (D), and E14.5 *Myf5*$^{nlacZ/nlacZ}$*:MyoD*$^{-/-}$ (B, F) embryos. *lacZ*-expressing cells strongly coexpress PCNA in *Myf5*$^{nlacZ/nlacZ}$*:MyoD*$^{-/-}$ forelimb (arrowheads in B and in the inset: the X-gal staining appears as a dark blue-turquoise rim around the nuclear red-brown immunostaining), but not in the *Myf5*^{nlacZ} heterozygous (A, arrowheads) or *258/−2.5lacZ* wild-type forelimb (C, arrowheads). In *258/− 2.5lacZ* double mutant embryos, coexpression of PCNA and β-galactosidase was a very rare observation (D, arrowheads). In both heterozygous and double mutant forelimbs *nlacZ*-expressing cells are not undergoing programmed cell death (E, F). However, a group of cells that does not express *nlacZ* is undergoing apoptosis in double mutant forelimb only (arrowheads in F and in the inset: the X-gal staining does not appear as a dark blue-turquoise rim around the nuclear red-brown immunostaining). Note that numerous *258/−2.5lacZ*-expressing nuclei appear apoptotic in double mutant forelimbs (D, arrows). Magnification, 400×, 1000× (insets).

cells were present and survive in *Myf5*$^{nlacZ/nlacZ}$ embryos (Tajbakhsh et al., 1996, 1997). We recently investigated the expression patterns of MyoD-*lacZ* transgenes in *Myf5*$^{-/-}$:*MyoD*$^{-/-}$ embryos and observed that *Myf5*- and *MyoD*-deficient presumptive muscle progenitor cells expressing β-galactosidase form and survive during several embryonic days in the absence of both primary MRFs (Kablar et al., 1999). To investigate whether myogenic precursor cells could acquire a myogenic fate during early stages of *Myf5*$^{-/-}$:*MyoD*$^{-/-}$ embryonic development, we studied the expression pattern of Myogenin-*lacZ* transgene and a panel of antibodies reactive with proteins present in either myogenic precursor cells (Myf5, MyoD, and MNF; Garry et al., 1997), myoblasts (Myogenin, nestin, and desmin), or differentiated myotubes (MHC). Consistently, we did not detect any of these markers in somites of *Myf5*$^{-/-}$:*MyoD*$^{-/-}$ E10.5 and E11.5 embryos, and we concluded that, in these double mutants, myogenic precursor cells could not undergo their normal developmental program that led to the acquisition of a myogenic fate.

We have recently reported an observation that the −20-kb *MyoD* enhancer activates expression in newly formed somites and limb buds in compound mutant embryos, suggesting that myogenic determination occurs independently in somites and limb buds (Kablar et al., 1999; Tajbakhsh and Buckingham, 2000). In addition, we have found that *Pax3* induction and the subsequent migration of myogenic precursors into the limb are unaffected by the absence of MRF expression (Kablar et al., 1999). However, *Myf5*$^{-/-}$:*MyoD*$^{-/-}$ embryonic forelimb buds did not stain with antibodies reactive with proteins present in myoblasts (Myogenin and desmin) or differentiated myotubes (MHC), and we concluded that, in these Myf5:MyoD mutants, myogenic precursor cells could not acquire myogenic fate even at the site of the de novo induction of *MyoD* transcription during development. We note, however, that in the *Myf5*$^{nlacZ/nlacZ}$ null, Mrf4 expression is compromised due to the insertion of foreign sequences in the *Myf5* locus (Tajbakhsh, 2002; S.T. and Buckingham, unpublished data). Therefore, we cannot exclude a myogenic role for Mrf4 in the absence of Myf5 and MyoD.

The precursor cells found in *Myf5*$^{-/-}$:*MyoD*$^{-/-}$ embryos (Kablar et al., 1998, 1999; B.K. and M.A.R., unpublished observation) could remain developmentally arrested, undergo programmed cell death, or change their fate (Tajbakhsh et al., 1996; Kablar et al., 1999). Recently, reported analysis reveals that MyoD-*lacZ*-expressing cells at the earlier embryonic ages (between E10.5 and E12.5) show similarly low apoptosis in the forelimbs of both wild-type and *Myf5*$^{-/-}$:*MyoD*$^{-/-}$ embryos (Kablar et al., 1999). In addition, double-labeling of matched wild-type and *Myf5*$^{-/-}$:*MyoD*$^{-/-}$ sections of E13.5 embryos with β-galactosidase and TUNEL reveals increased levels of programmed cell death of cells stained with *258/−2.5lacZ* in mutant embryos, suggesting that by E13.5, many of these *lacZ*-expressing cells are eliminated by programmed cell death (Kablar et al., 1999). However, the more accurate whole-mount in situ TUNEL detection revealed that, at both sites of myogenic determination, the dermomyotome and the forelimbs, increased levels of programmed cell death was observed in *Myf5*$^{-/-}$:*MyoD*$^{-/-}$ E10.5 embryos. Taken together, it appears that, from the early stages of muscle development, apoptosis (on E10.5) eliminates a portion of myogenic precursor cells at both sites of myogenic determination, the dermomyotome and the forelimbs. Moreover, it appears that, at this early stage, apoptosis partially eliminates Myf5-positive cells in the absence of Myf5 and MyoD, while at later stages (on E13.5), apoptosis eliminates MyoD-*lacZ*-expressing myogenic precursor cells. In support of this hypothesis are findings that *Myf5*^{nlacZ}-expressing cells in the forelimbs of E14.5 compound-mutant embryos did not undergo apoptosis and instead coexpressed PCNA, whereas some adjacent cells which may be MyoD-dependent at this stage were destined to die. These findings highlight the differential roles of Myf5- and MyoD-expressing cells. At late stages, it is possible that Myf5 downregulation and continued MyoD expression represent a more "downstream" myogenic cell which would subsequently undergo apoptosis. The susceptibility of the cell to undergo apoptosis my also be related to the signals received by that cell, as reflected by the differential activation of the Myf5 and MyoD regulatory elements.

Analysis of muscle development in embryos harboring null mutations in either *Myf5* or *MyoD* genes, reveals that Myf5 and MyoD are not redundant, but that each controls the early determination of a distinct muscle cell compartment (Kablar et al., 1997, 1998). Based on these studies, diversity among myogenic precursor cells is hypothesized to exist from early stages of embryonic development, resulting in two coexisting Myf5- and MyoD-dependent myogenic precursor cell lineages. Detailed analysis of *258/−2.5lacZ* (−20 kb enhancer of *MyoD*) embryos (Kablar et al., 1999) and the analysis of *Myf5*^{nlacZ} embryos (Tajbakhsh et al., 1996) indicated that, in the absence of both Myf5 and MyoD, muscle progenitor cells indeed existed, delaminated from the dermamyotome to become mesenchymal and remained multipotential.

During later developmental stages, striking differences in fate were found between *258/−2.5lacZ*- and *Myf5*^{nlacZ}-expressing cells in double mutant background. The MyoD-*lacZ*-expressing cells were found to undergo cell death from E13.5, while *Myf5*^{nlacZ}-expressing cells continued to proliferate (e.g., coexpress PCNA and β-galactosidase) and therefore remained developmentally arrested (on E14.5). One possibility is that separate lineages activate these genes (Braun and Arnold, 1996). For instance, using targeted inactivation of Myf5 and MyoD, it was shown that the two MRFs are not expressed in the same muscle precursor cell in an in vitro embryonic stem (ES) derived system, and that their expression pattern determines different muscle cell lineages originating from different myogenic precursor cell populations. Another interpretation is that different signals

preferentially activate (Cossu et al., 1996; Tajbakhsh et al., 1998) and maintain their expression. For instance, by employing cultures of paraxial mesoderm with a variety of adjacent structures, it was demonstrated that the neural tube activates myogenesis through a *Myf5*-dependent pathway, whereas the dorsal ectoderm activates myogenesis through a *MyoD*-dependent pathway. To distinguish between these possibilities, one would need to generate a *MyoD* knock-in mouse expressing a transgene other than *lacZ* (e.g., alkaline phosphatase), that can be subsequently bred with the *Myf5*^{nlacZ} knock-in mouse in order to obtain embryos expressing both transgenes.

In conclusion, we show in vivo that myogenic precursor cells are not capable of acquiring a myogenic phenotype in these *Myf5:MyoD* mutants, even at later stages. Instead, these cells can remain either developmentally arrested for an extended period, change their fate, or undergo programmed cell death.

Acknowledgments

M.A.R. is a Research Scientist of the Medical Research Council of Canada, and a member of the Canadian Genetic Disease Network of Excellence. We thank Chuyan Ying and Anne C. Belliveau for expert technical assistance. This work was supported by a grant from the Medical Research Council of Canada (to M.A.R.), by a grant from the Human Frontiers (to M.A.R. and S.T.), and by a grant from the Natural Sciences and Engineering Research Council (NSERC) of Canada and The Hospital for Sick Children Foundation (HSCF) research grant (to B.K.).

References

Bader, D., Masaki, T., Fischmann, D.A., 1982. Immunohistochemical analysis of myosin heavy chain during myogenesis in vivo and in vitro. J. Cell Biol. 95, 763–770.

Bischoff, R., 1994. The satellite cell and muscle regeneration, in: Engel, A.G., Franzini-Armstrong, C. (Eds.), Myology, 2nd ed., McGraw-Hill, New York, pp. 97–133.

Braun, T., Rudnicki, M.A., Arnold, H.H., Jaenisch, R., 1992. Targeted inactivation of the muscle regulatory gene *myf-5* results in abnormal rib development and perinatal death. Cell 71, 369–382.

Braun, T., Arnold, H.H., 1996. Myf-5 and myoD genes are activated in distinct mesenchymal stem cells and determine different skeletal muscle cell lineage. EMBO J. 15, 310–318.

Cheng, T.-C., Wallace, M.C., Merlie, J.P., Olson, E.N., 1993. Separable regulatory elements governing *Myogenin* transcription in mouse embryogenesis. Science 261, 215–218.

Christ, B., Ordahl, C.P., 1995. Early stages of chick somite development. Anat. Embryol. 191, 381–396.

Cossu, G., Kelly, R., Tajbakhsh, S., Di Donna, S., Vivarelli, E., Buckingham, M., 1996. Activation of different myogenic pathways: myf-5 is induced by the neural tube and MyoD by the dorsal ectorerm in mouse paraxial mesoderm. Development 122, 429–437.

Cserjesi, P., Brown, D., Ligon, K.L., Lyons, G.E., Copeland, N.G., Gilbert, D.J., Jenkins, N.A., Olson, E.N., 1995. Scleraxis: a basic helix–loop–helix protein that prefigures skeletal formation during mouse embryogenesis. Development 121, 1099–1110.

Faerman, A., Goldhamer, D.J., Puzis, R., Emerson, C.P., Shani., M., 1995. The distal human myoD enhancer sequences direct unique muscle-specific patterns of lacZ expression during mouse development. Dev. Biol. 171, 27–38.

Garry, D.J., Yang, Q., Bassel-Duby, R., Williams, R.S., 1997. Persistent expression of MNF identifies myogenic stem cells in postnatal muscles. Dev. Biol. 188, 280–294.

Gavrieli, Y., Sherman, Y., Ben-Sasson, S.A., 1992. Identification of programmed cell death in situ via specific labeling of nuclear DNA fragmentation. J. Cell Biol. 119, 493–501.

Glant, T.T., Mikecz, K., Roughley, P.J., Buzas, E., Poole, A.R., 1986. Age-related changes in protein-related epitopes of human articular-cartilage proteoglycans. Biochem. J. 236, 71–75.

Goldhamer, D.J., Faerman, A., Shani, M., Emerson, C.P., 1992. Regulatory elements that control the lineage-specific expression of myoD. Science 256, 538–542.

Goldhamer, D.J., Brunk, B.P., Faerman, A., King, A., Shani, M., Emerson, C.P., 1995. Embryonic activation of the MyoD gene is regulated by a highly conserved distal control element. Development 121, 637–649.

Hasty, P., Bradley, A., Morris, J., Edmondson, D., Venuti, J., Olson, E., Klein, W., 1993. Muscle deficiency and neonatal death in mice with a targeted mutation in the *myogenin* gene. Nature 364, 501–506.

Hauschka, S.D., 1994. The embryonic origin of muscle, in: Engel, A.G., Franzini-Armstrong, C. (Eds.), Myology, 2nd ed, McGraw-Hill, New York, pp. 3–73.

Kablar, B., Krastel, K., Ying, C., Asakura, A., Tapscott, S.J., Rudnicki, M.A., 1997. *MyoD* and *Myf-5* differentially regulate the development of limb versus trunk skeletal muscle. Development 124, 4729–4738.

Kablar, B., Asakura, A., Krastel, K., Ying, C., May, L.L., Goldhamer, D.J., Rudnicki, M.A., 1998. MyoD and Myf-5 define the specification of musculature of distinct embryonic origin. Biochem. Cell Biol. 76, 1079–1091.

Kablar, B., Rudnicki, M.A., 1999. Development in the absence of skeletal muscle results in the sequential ablation of motor neurons from the spinal cord to the brain. Dev. Biol. 208, 93–109.

Kablar, B., Krastel, K., Ying, C., Tapscott, S.J., Goldhamer, D.J., Rudnicki, M.A., 1999. Myogenic determination occurs independently in somites and limb buds. Dev. Biol. 206, 219–231.

Kablar, B., Rudnicki, M.A., 2000. Skeletal muscle development in the mouse embryo. Histol. Histopathol. 15, 649–656.

Laird, P.W., Zijderveld, A., Linders, K., Rudnicki, M.A., Jaenish, R., Berns, A., 1991. Simplified mammalian DNA isolation procedure. Nucleic Acids Res. 19, 4293.

Li, L., Cserjesi, P., Olson, E.N., 1995. Dermo-1: a novel twist-related bHLH protein expressed in the developing dermis. Dev. Biol. 172, 280–292.

Megeney, L.A., Rudnicki, M.A., 1995. Determination versus differentiation and the MyoD-family of transcription factors. Biochem. Cell Biol. 73, 723–732.

Molkentin, J.D., Olson, E.N., 1996. Defining the regulatory networks for muscle development. Curr. Opin. Genet. Dev. 6, 445–453.

Nabeshima, Y., Hanaoka, K., Hayasaka, M., Esumi, E., Li, S., Nonaka, I., Nabeshima, Y., 1993. *Myogenin* gene disruption results in perinatal lethality because of severe muscle defect. Nature 364, 532–535.

Ordahl, C.P., Le Dourain, N., 1992. Two myogenic cell lineages within the developing somite. Development 114, 339–353.

Ordahl, C.P., Williams, B.A., 1998. Knowing chops from chuck: roasting MyoD redundancy. BioEssays 20, 357–362.

Rudnicki, M.A., Braun, T., Hinuma, S., Jaenisch, R., 1992. Inactivation of *MyoD* in mice leads to up-regulation of the myogenic HLH gene *Myf-5* and results in apparently normal muscle development. Cell 71, 383–390.

Rudnicki, M.A., Schnegelsberg, P.N.J., Stead, R.H., Braun, T., Arnold, H.H., Jaenish, R., 1993. MyoD or Myf-5 is required for the formation of skeletal muscle. Cell 75, 1351–1359.

Rudnicki, M.A., Jaenish, R., 1995. The MyoD family of transcription factors and skeletal myogenesis. BioEssays 17, 203–209.

Sambrook, J., Fritsch, E.F., Maniatis, T., 1989. Molecular Cloning: A Laboratory Manual, Nolan, C. (Ed.), Cold Spring Harbor Laboratory Press, Cold Spring Harbor, NY.

Sassoon, D., Lyons, G., Wright, W.E., Lin, V., Lassar, A., Weintraub, H., Buckingham, M., 1989. Expression of two myogenic regulatory factors, myogenin and MyoD1, during mouse embryogenesis. Nature 341, 303–307.

Tajbakhsh, S., Buckingham, M., 1994. Mouse limb muscle is determined in the absence of the earliest myogenic factor *myf-5*. Proc. Natl. Acad. Sci. USA 91, 747–751.

Tajbakhsh, S., Rocancourt, D., Buckingham, M., 1996. Muscle progenitor cells failing to respond to positional cues adopt non-myogenic fates in myf-5 null mice. Nature 384, 266–270.

Tajbakhsh, S., Rocancourt, D., Cossu, G., Buckingham, M., 1997. Redefining the genetic hierarchies controlling skeletal myogenesis: Pax-3 and Myf-5 act upstream of MyoD. Cell 89, 127–38.

Tajbakhsh, S., Spörle, R., 1998. Somite development: constructing the vertebrate body. Cell 92, 9–16.

Tajbakhsh, S., Borello, U., Vivarelli, E., Kelly, R., Papkoff, J., Dupez, D., Buckingham, M., Cossu, G., 1998. Differential activation of Myf5 and MyoD by different Wnts in explants of mouse paraxial mesoderm and the later activation of myogenesis in the absence of Myf5. Development 125, 4155–4162.

Tajbakhsh, S., Buckingham, M., 2000. The birth of muscle progenitor cells in the mouse: spatiotemporal considerations. Curr. Top. Dev. Biol. 48, 225–268.

Tajbakhsh, S., 2002. The genetics of murine skeletal muscle biogenesis, in: Brand-Saberi, B. (Ed.), Results and Problems in Cell Differentiation: Vertebrate Myogenesis, Vol. 38, Springer-Verlag, Berlin, pp. 61–79.

Wachtler, F., Christ, B., 1992. The basic embryology of skeletal muscle formation in vertebrates: the avian model. Semin. Dev. Biol. 3, 217–227.

Wang, Y., Schnegelsberg, P.N.J., Dausman, J., Jaenish, R., 1996. Functional redundancy of the muscle-specific transcription factors Myf5 and myogenin. Neture 379, 823–825.

Weintraub, H., 1993. The myoD family and myogenesis: redundancy, networks and tresholds. Cell 75, 1241–1244.

Wilkinson, D.G., 1992. In Situ Hybridisation: A Practical Approach, Wilkinson, D.G. (Ed.), IRL Press, Oxford.

Zhang, W., Behringer, R.R., Olson, E.N., 1995. Inactivation of the myogenic bHLH gene *MRF4* results in upregulation of myogenin and rib anomalies. Genes Dev. 9, 1388–1399.